ON THE ENVIRONMENTAL DEPENDENCE OF THE CLUSTER GALAXY ASSEMBLY TIMESCALE

C. CARRETERO,[1] A. VAZDEKIS,[1] J. E. BECKMAN,[1,2] P. SÁNCHEZ-BLÁZQUEZ,[3] AND J. GORGAS[3]

ABSTRACT

We present estimates of CN and Mg overabundances with respect to Fe for early-type galaxies in eight clusters over a range of richness and morphology. Spectra were taken from the Sloan Digital Sky Survey Data Release 1 and from William Hershel Telescope and Centro Astronómico Hispano-Alemán observations. Abundances were derived from absorption lines and single-burst population models, by comparing galaxy spectra with appropriately broadened synthetic model spectra. We detect correlations between the [Mg/CN] and [CN/Fe] values and the cluster X-ray luminosity. No correlation is observed for [Mg/Fe]. We also see a clear trend in the richness and morphology of the clusters. This is interpreted as giving varying formation timescales for CN, Mg, and Fe and a varying star formation history in early-type galaxies as a function of their environment: intermediate-mass early-type galaxies in more massive clusters are assembled on shorter timescales than in less massive clusters, with an upper limit of ~1 Gyr.

Subject headings: cosmology: observations — galaxies: abundances — galaxies: clusters: general — galaxies: formation — galaxies: stellar content — X-rays: galaxies: clusters

1. INTRODUCTION

A key question for scenarios of galaxy formation is whether galaxies formed in single structural "monolithic" events (Larson 1974) or by a series of "hierarchical" processes (Press & Schechter 1974; White & Frenk 1991) in which large galaxies were built up from smaller ones. Many structural and dynamical properties of galaxies in clusters are explained by the hierarchical scenario, although problems remain: the absence of the predicted mass cusps in the centers of elliptical galaxies and bulges and the prediction of far more satellite galaxies than those observed.

Stellar populations offer a fossil record of the formation and evolution of galaxies, most clearly in elliptical galaxies, and stellar population studies provide very strong constraints on the principal galaxy formation scenarios. It is hard to reconcile the hierarchical models with the result that massive galaxies show significantly larger mean luminosity-weighted ages than their smaller counterparts (Kauffmann et al. 2003).

Understanding stellar populations in early-type galaxies as a function of the environment can provide answers to the puzzle. The present observational base is small. Only three clusters have been observed for a detailed stellar populations analysis: Virgo (e.g., Vazdekis et al. 2001b), Coma (e.g., Jørgensen 1999), and Fornax (Kuntschner & Davies 1998). Extending the study to a large number of clusters covering a range of richness and morphology is mandatory.

Past studies of clusters used the original Lick/IDS spectral indices (Worthey 1994) whose reliability is limited by their resolution dependence, as uncertain corrections for broadening and instrumental effects are needed. It is better to use modeled integrated spectra, which can be broadened to match the galaxy velocity dispersion, σ. Such models have been developed by Vazdekis (1999) and allow one to accurately separate age and metallicity and to make subsequent individual abundance derivations.

[1] Instituto de Astrofísica de Canarias, Vía Láctea s/n, 38200 La Laguna, Tenerife, Spain; cch@iac.es.

[2] Consejo Superior de Investigaciones Científicas, Spain.

[3] Departamento de Astrofísica, Facultad de Físicas, Universidad Complutense de Madrid, 28040 Madrid, Spain.

The study of the element abundance ratios in elliptical galaxies within distinct clusters should be a powerful discriminant between different star formation histories (e.g., Worthey 1998). In particular, overabundances of [Mg/Fe] compared with the solar ratio have been found in massive elliptical galaxies (Peletier 1989; Worthey et al. 1992; Vazdekis et al. 1997). These galaxies have been interpreted via several possible scenarios based on the fact that Mg is mainly produced in Type II supernovae (SNe II; Faber et al. 1992; Matteucci 1994), and they include different star formation rates and a time-dependent initial mass function (IMF).

Differences in the abundances of C and N as a function of the environment have been recently suggested by Sánchez-Blázquez et al. (2003), who found striking spectral differences between field elliptical galaxies and their counterparts in the central region of the Coma Cluster. Galaxies in the denser environment showed significantly lower CN_2 and C4668 absorption strength. Here we explore these differences by extending the study to a larger number of clusters over a range of richness and morphology, applying the new analysis techniques to derive abundance ratios. We have assumed a flat universe with $H_0 = 75$ km s^{-1} Mpc^{-1} and $q_0 = 0.5$.

2. DATA

Sloan Digital Sky Survey (SDSS; Stoughton et al. 2002) spectra were obtained using a multiobject, $3''$ diameter fiber spectrograph. Exposures ranged from 45 to 75 minutes. All the data processing was performed with automated SDSS software. Redshifts were measured on the reduced spectra by an automated system, which models each galaxy spectrum as a linear combination of stellar populations. We measured independently the redshifts of the galaxies used in this study by cross-correlating each galaxy spectrum with our simple stellar populaton synthetic model spectra. We found no significant differences between the SDSS redshift values and our own.

From the SDSS Data Release 1 database, we selected galaxy spectra according to the following criteria:

1. They must belong to an Abell cluster. We included this criterion because the richness and the morphology of Abell

TABLE 1
PROPERTIES AND MEASUREMENTS OF ANALYZED CLUSTERS

Cluster	z	Abell Richness Class	Bautz-Morgan Morphological Type	L_X $(10^{44}$ ergs s$^{-1})$	$[Z_{CN}/Z_{Fe}]$	$[Z_{Mg}/Z_{Fe}]$
A0279	0.080	1	II–III	0.08	0.43	0.33
A1238	0.073	1	III	0.15	0.61	0.44
Virgo	0.004	1	III	0.30	0.48	0.36
A0257	0.070	1	II–III	0.31	0.45	0.35
A2050	0.118	1	II–III	1.22	0.40	0.31
Coma	0.023	2	II	1.80	0.39	0.38
A0655	0.127	3	I–II	1.97	0.30	0.43
A1650	0.085	2	I–II	2.01	0.40	0.39

clusters are uniformly defined and described in the literature. Also, X-ray luminosity values are available.

2. They must belong to the early-type galaxy catalog of Bernardi et al. (2003). This sample has ~9000 early-type galaxies, in the redshift range $0.01 \leq z \leq 0.3$, selected from the SDSS spectroscopic database using morphological and spectral criteria. The mean spectrum signal-to-noise ratio (S/N) per pixel is 16.

3. They must have an S/N per pixel greater than 15.

4. They must have a velocity dispersion in the range 150 km s^{-1} $\leq \sigma \leq$ 250 km s^{-1}. Galaxies outside this range of σ were rejected because of the completeness of the sample: not all clusters had spectra of dwarf and/or giant elliptical galaxies, because of the inner limitation of SDSS data (for dwarfs) and/

or because of the morphology of the clusters (for giants). Also, the quality of the spectra of the faintest galaxies was too low for our analysis requirements; σ-values were obtained from Bernardi et al. (2003).

Using these criteria, we obtained a total of 55 galaxies distributed in six clusters. The clusters are A257, A279, A655, A1238, A1650, and A2050. Their redshift values vary in the range $0.07 < z < 0.13$, and they cover a range of richness and morphology. See details in Table 1.

For comparison and completeness, we added high-quality long-slit spectra of early-type galaxies in the Coma and Virgo Clusters (for details, see Sánchez-Blázquez et al. 2003) to our SDSS data. To compare them with those of the SDSS sample, we extracted spectra along the slit simulating a circular aperture (distance-weighted co-added spectra) of radius 1″.5 at $z =$ 0.1. This aperture translates into apertures of radius 6″ for Coma and 37″ for Virgo.

3. GALAXY MEASUREMENTS AND RESULTS

To derive mean luminosity-weighted ages and metallicities, we compared selected absorption-line strengths with those predicted by the model of Vazdekis (1999). This model provides flux-calibrated spectra in the optical range at a resolution of 1.8 Å (FWHM) for single-burst stellar populations. This way, we can transform synthetic spectra to the resolution and dispersion of the galaxy spectra instead of the opposite, as required while working in the Lick system. Selected absorption indices were CN_2, Mg_2 (Worthey et al. 1994), and Fe2 [defined as Fe2 = (Fe4383 + Fe5270) /2]. We used these features because of their low sensitivity to variations in S/N (Cardiel et al. 2003) and velocity dispersion [we have estimated Δ(index)/index < 0.15, for $\Delta(\sigma)$ = 300 km s^{-1}]. This way we avoid possible variations in the index value, as σ may vary as a function of r, due to the fact that SDSS spectra provide the light integrated within the fibers of the spectrograph.

Plots of the strengths of the selected indices versus Hβ provide close to orthogonal model grids, allowing us to estimate accurately the galaxy mean ages as well as the relative abundances of the different elements. Figure 1 illustrates this method for the galaxies of clusters A1238 and A655 (two clusters with extreme values of X-ray luminosity). We will refer to the metallicities derived in the diagrams CN_2–Hβ, Mg_2–Hβ, and Fe2–Hβ as Z_{CN}, Z_{Mg}, and Z_{Fe}, respectively. Since the CN_2 index is strongly dominated by C and N, the Mg_2 index is governed by Mg, and the Fe2 index by Fe (Tripicco & Bell 1995), these metallicities must be close to the [CN/H], [Mg/H], and [Fe/H] abundances, and $[Z_{CN}/Z_{Fe}]$, $[Z_{Mg}/Z_{Fe}]$, and $[Z_{Mg}/Z_{CN}]$ are then estimates of the abundance ratios [CN/Fe], [Mg/Fe], and [Mg/CN] for each galaxy. Note that an extrapolation of the model
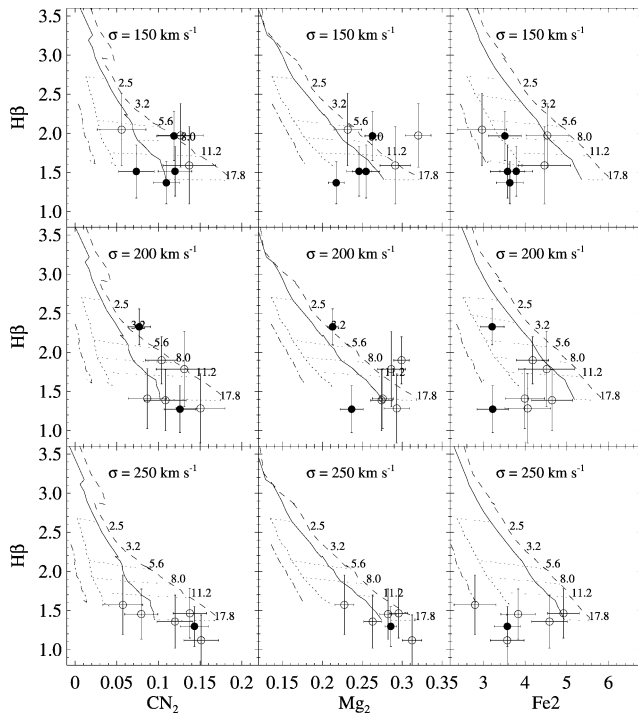

FIG. 1.—Model grids for the galaxies of clusters A1238 (*filled circles*) and A655 (*open circles*). These two clusters have extreme values of X-ray luminosity. *From left to right:* Plots of Hβ vs. the metallicity indices CN_2, Mg_2, and Fe2 (defined in the text). The galaxy velocity dispersions increase from top to bottom, in the three bins of σ quoted in the boxes, to which galaxy and model spectra have been broadened. Overplotted are the models by Vazdekis (1999). Lines of constant [Fe/H] = −0.7, −0.4, 0.0, and 0.2 are shown by dot-dashed, dotted, solid, and dashed lines, respectively. Thin dotted horizontal lines represent models of constant age, quoted in gigayears. The ages become increasingly uncertain for values greater than 8 Gyr (see Worthey 1994 and Vazdekis 1999), but these uncertainties have no significant effects on the relative abundance determination.
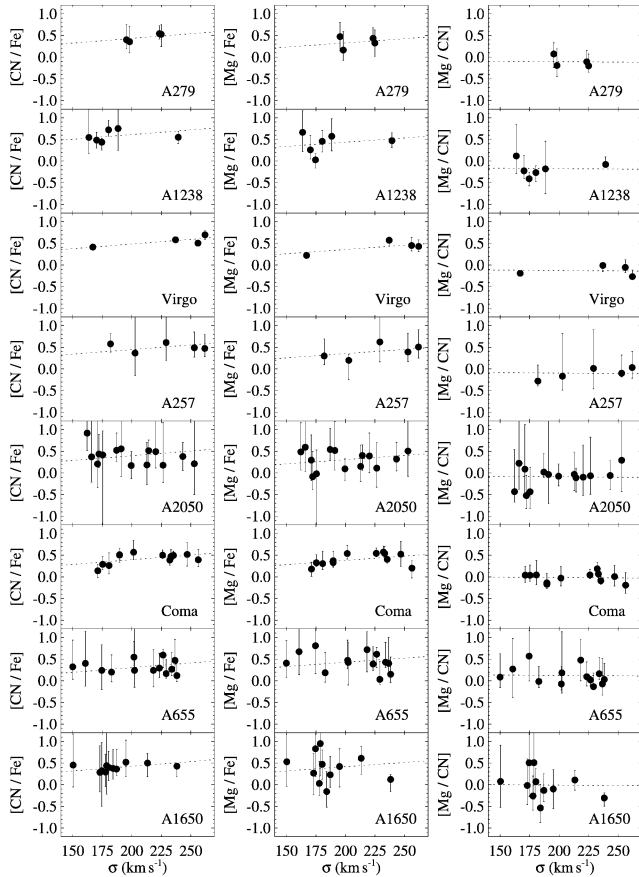
Fig. 2.—Abundance ratios $[Z_{CN}/Z_{Fe}]$ (*left*), $[Z_{Mg}/Z_{Fe}]$ (*middle*), and $[Z_{Mg}/Z_{CN}]$ (*right*) vs. galaxy velocity dispersion, σ. Each point corresponds to one galaxy within a cluster. Errors are computed from the measured index error bars shown in Fig. 1. Galaxy clusters are ordered by decreasing X-ray luminosity, from top to bottom. The dotted straight lines show the level of relative abundances for each cluster. See the text for more details.

Fig. 3.—Cluster X-ray luminosity vs. overabundance values of $[Z_{CN}/Z_{Fe}]$ (*top*), $[Z_{Mg}/Z_{Fe}]$ (*middle*), and $[Z_{Mg}/Z_{CN}]$ (*bottom*). Circles, squares, and triangles indicate clusters with richness classes of 1, 2, and 3, respectively. Each point corresponds to one individual cluster and represents the interpolated abundance ratio for $\sigma = 200$ km s^{-1}. The Spearman rank-order correlation coefficients and its significance values are labeled in the top and bottom panels.

grids is required for some galaxies to obtain the abundances of CN and Mg, since the models extend only to [M/H] = 0.2. It is worth noting that certain galaxies fall below the model grids, which can be attributed to the fact that absolute age determination is subject to model uncertainties (see Vazdekis et al. 2001a and Schiavon et al. 2002). We neglect the possible effect of nebular emission on Hβ since no [O III] $\lambda5007$ emission is detected in our galaxy spectra. Nevertheless, assuming an upper Hβ emission correction of ~0.5 Å (Kuntschner et al. 2002), although this would give rise to a significant reduction in the mean age of the stellar populations of the oldest galaxies, the net effect on the abundance ratios would be no more than ~0.05 dex, for the most affected galaxies in a cluster. Note that this correction for the Hβ index is larger than the one obtained by varying the model prescriptions, e.g., with α-enhanced isochrones and atomic diffusion included (Vazdekis et al. 2001a), for inferring ages in better agreement with the current age of the universe, for the oldest galaxies in our sample. However, we do recognize that the ages quoted here, and in current articles dealing with stellar population modeling, may well span an older range than the true age range of the populations observed. This would indicate some flaw or flaws in the present quantitative understanding of stellar evolution and is a problem recognized by the community working in population synthesis.

Figure 2 shows the measured abundance ratios for the galaxies in the whole sample of clusters as a function of the velocity dispersion. Since relative abundances correlate with
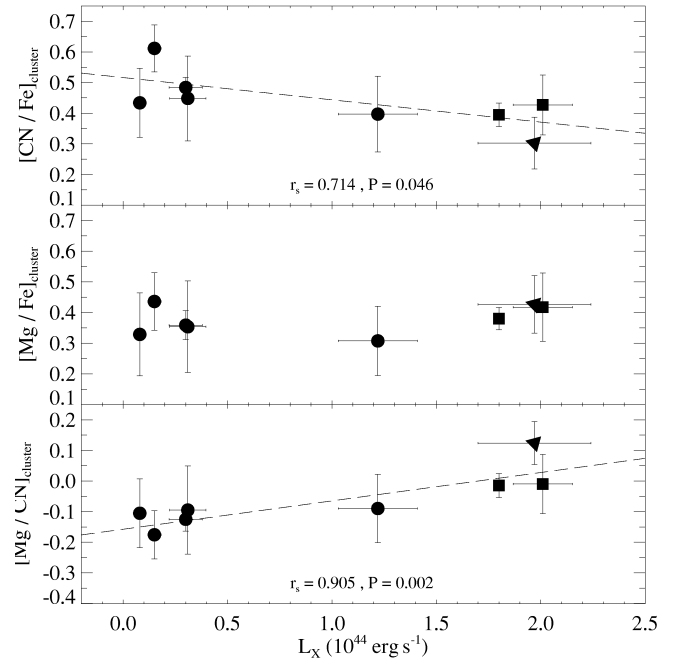
σ, to derive representative relative abundance ratios for each cluster, we have fitted to each cluster a straight line with a fixed slope and a varying intercept. We have assumed that this slope corresponds to that found for the Coma Cluster in the considered range of σ. Note that we do not have any statistically significant evidence of a variation of the slope between the different clusters. In Table 1 we list the derived relative abundances at a fixed velocity dispersion of $\sigma = 200$ km s^{-1} for each cluster.

As a quantitative indicator of the masses of the clusters, we have used X-ray luminosities. L_X-values were taken from Ebeling et al. (1998) and Ledlow et al. (2003), adapted to the cosmological parameters used by the latter.

Figure 3 shows the values of $[Z_{CN}/Z_{Fe}]$, $[Z_{Mg}/Z_{Fe}]$, and $[Z_{Mg}/Z_{CN}]$ versus X-ray luminosity for each cluster. We find clear correlations between the [CN/Fe] and [Mg/CN] values and X-ray luminosity, with probabilities of 0.046 and 0.002, respectively, of no correlation. On the contrary, no correlation is found for [Mg/Fe]. It is worth noting that the significant point in these relations is the relative differences in abundance ratios, not their absolute values. It is noticeable that the abundance ratio values also correlate with the richness class and the morphological type (see Table 1), with probabilities of 0.05 and 0.02, respectively, of no correlation.

4. DISCUSSION

The correlations can be interpreted in terms of the different formation timescales for each element and the different star formation histories of early-type galaxies as a function of their environment. Magnesium is ejected into the interstellar medium (ISM) by SNe II on short timescales (<10 Myr). On the other hand, the iron-peak elements are the products of SNe Ia, which occur on timescales of ~1 Gyr. Between the two extremes,

CARRETERO ET AL.

although there are recent suggestions that most of the C come from massive stars (Akerman et al. 2004), C and N are mainly ejected into the ISM by low- and intermediate-mass stars (Renzini & Voli 1981; Chiappini et al. 2003), leading to CN formation on timescales longer than for Mg but shorter than for Fe. Furthermore, several authors (e.g., Ellis et al. 1997; Stanford et al. 1998) argue that early-type galaxies are old and passively evolving systems. In any case, the luminosity-weighted ages derived from our model grids confirm that the galaxies are significantly older than the formation timescales of the different species. So, if we find substantial differences in the abundance ratios of these elements that depend on the physical properties of the environment, these must be due to the fact that galaxies are assembled on different timescales as a function of their environment.

In this framework, the constancy of the [Mg/Fe]-values is explained in terms of the great difference in the formation timescales of the two elements: the galaxies are fully assembled before SNe Ia can significantly pollute with Fe the ISM of the smaller galaxies before merging and right after Mg is fully ejected. Since [Mg/Fe] is found to be constant with the X-ray luminosity of the clusters (see Fig. 3), which is an indicator of their mass, we conclude that this ratio is independent of the environment. Similar results for the [Mg/Fe] ratio have been obtained by other authors (Jørgensen 1999; Kuntschner et al. 2002; Sánchez-Blázquez et al. 2003), by studying field and Coma Cluster elliptical galaxies.

However, when considering species with less disparate formation timescales, such as CN and Fe or CN and Mg, clear correlations are found between abundance ratios and the environment, as shown in Figure 3. The fact that [CN/Fe] decreases with the cluster X-ray luminosity, and [Mg/CN] increases with it, suggests that galaxies in more massive clusters are fully assembled on shorter timescales than those in less massive clusters. We show that this difference is large enough to produce measurable variations of the abundance ratios of galaxies in more or less massive clusters.

The result that there exist relative differences in the assembly timescales of the galaxies due to the properties of the environment is qualitatively in agreement with the hierarchical models. Discrepancies appear, however, when considering the absolute values of such timescales. The fact that the [CN/Fe] abundance ratio is not constant implies that early-type galaxies are fully assembled on timescales around the massive release of CN into the ISM. Hierarchical models, on the contrary, predict longer assembly timescales.

Other scenarios have been explored in order to explain the differences in abundance ratio values as functions of the environment (see Sánchez-Blázquez et al. 2003). These include a decrease in the stellar giant/dwarf ratio in high-density environments, with respect to low-density ones, which would lead to lower index values in the latter. But model calculations have shown that the differences due to a variation in the IMF are too small to produce the observed variations. Also, a difference in the luminosity-weighted mean age between high- and low-density environments has been proposed. Models show that, to account for the differences, the galaxies in high-density environments must be ~8 Gyr younger than in low-density ones. This contradicts previous studies that suggest that galaxies in high-density environments are, in any case, older than those in low-density environments (Kuntschner et al. 2002). So our interpretation here seems the most consistent.

It is noteworthy that we have found the abundance ratios to be dependent on several properties of the environment, both quantitatively (i.e., X-ray luminosity values) and qualitatively (i.e., richness and morphological types) as shown in Table 1. This lends strong support to the basic hypothesis that the characteristics of the environment affect the evolution of the galaxies. The relations we have found set clear constraints on models of chemical evolution and galaxy formation.

REFERENCES

Akerman, C. J., Carigi, L., Nissen, P. E., Pettini, M., & Asplund, M. 2004, A&A, 414, 931
Bernardi, M., et al. 2003, AJ, 125, 1817
Cardiel, N., Gorgas, J., Sánchez-Blázquez, P., Cenarro, A. J., Pedraz, S., Bruzual, G., & Klement, J. 2003, A&A, 409, 511
Chiappini, C., Romano, D., & Matteucci, F. 2003, MNRAS, 339, 63
Ebeling, H., Edge, A. C., Böhringer, H., Allen, S. W., Crawford, C. S., Fabian, A. C., Voges, W., & Huchra, J. P. 1998, MNRAS, 301, 881
Ellis, R. S., Smail, I., Dressler, A., Couch, W. J., Oemler, A. J., Butcher, H., & Sharples, R. M. 1997, ApJ, 483, 582
Faber, S. M., Worthey, G., & González, J. J. 1992, in IAU Symp. 149, Stellar Populations of Galaxies, ed. B. Barbury & A. Renzini (Dordrecht: Kluwer), 255
Jørgensen, I. 1999, MNRAS, 306, 607
Kauffmann, G., et al. 2003, MNRAS, 341, 54
Kuntschner, H., & Davies, R. L. 1998, MNRAS, 295, L29
Kuntschner, H., Smith, R., Colles, M., Davies, R., Kaldare, R., & Vazdekis, A. 2002, MNRAS, 337, 172
Larson, R. B. 1974, MNRAS, 166, 585
Ledlow, M. J., Voges, W., Owen, F. N., & Burns, J. O. 2003, AJ, 126, 2740
Matteucci, F. 1994, A&A, 288, 57
Peletier, R. F. 1989, Ph.D. thesis, Univ. Groningen

Press, W. H., & Schechter, P. 1974, ApJ, 187, 425
Renzini, A., & Voli, M. 1981, A&A, 94, 175
Sánchez-Blázquez, P., Gorgas, J., Cardiel, N., Cenarro, J., & González, J. J. 2003, ApJ, 590, L91
Schiavon, R. P., Faber, S. M., Castilho, B. V., & Rose, J. A. 2002, ApJ, 580, 850
Stanford, S. A., Eisenhardt, P., & Dickinson, M. 1998, ApJ, 492, 461
Stoughton, C., et al. 2002, AJ, 123, 485
Tripicco, M., & Bell, R. A. 1995, AJ, 110, 3035
Vazdekis, A. 1999, ApJ, 513, 224
Vazdekis, A., Kuntschner, H., Davies, R., Arimoto, N., Nakamura, O., & Peletier, R. 2001a, ApJ, 551, L127
Vazdekis, A., Peletier, R. F., Beckman, J. E., & Casuso, E. 1997, ApJS, 111, 203
Vazdekis, A., Salaris, M., Arimoto, N., & Rose, J. A. 2001b, ApJ, 549, 274
White, S. D. M., & Frenk, C. S. 1991, ApJ, 379, 52
Worthey, G. 1994, ApJS, 95, 107
———. 1998, PASP, 110, 888
Worthey, G., Faber, S. M., & González, J. J. 1992, ApJ, 398, 69
Worthey, G., Faber, S. M., González, J. J., & Burstein, D. 1994, ApJS, 94, 687